The Function of Intermediate Filaments in Cell Shape and Cytoskeletal Integrity

Robert D. Goldman,* Satya Khuon,* Ying Hao Chou, Puneet Opal,* and Peter M. Steinert‡

*Department of Cell and Molecular Biology, Northwestern University Medical School, Chicago, Illinois 60611; and‡Laboratory for Skin Biology, National Institute of Arthritis, Musculoskeletal, and Skin Diseases/National Institutes of Health, Bethesda, Maryland 20892-2755

Abstract. This study describes the development and use of a specific method for disassembling intermediate filament (IF) networks in living cells. It takes advantage of the disruptive effects of mimetic peptides derived from the amino acid sequence of the helix initiation 1A domain of IF protein chains. The results demonstrate that at 1:1 molar ratios, these peptides disassemble vimentin IF into small oligomeric complexes and monomers within 30 min at room temperature in vitro. Upon microinjection into cultured fibroblasts, these same peptides induce the rapid disassembly of IF networks. The disassembly process is accompanied by a dramatic alteration in cell shape and the destabilization of microtubule and actin-stress fiber networks. These changes in cell shape and IF assembly states are reversible. The results are discussed with respect to the roles of IF in cell shape and the maintenance of the integrity and mechanical properties of the cytoplasm, as well as the stability of the other major cytoskeletal systems.

INTERMEDIATE filaments (IF)[1] are major fibrous proteins that are found in the nucleoplasm and the cytoplasm of most types of animal cells. In the cytoplasm, they are usually organized into complex arrays of 10-nm diameter cytoskeletal IF that are prevalent in the perinuclear region, where they frequently form a cage that surrounds and appears to position the nucleus. In this region, individual IF appear to be attached to the outer nuclear envelope membrane or to nuclear pore complexes (Skalli and Goldman, 1991). Continuous with this perinuclear array, IF extend radially through the cytoplasm, eventually forming close associations with the cell surface. Frequently, these membrane associations are concentrated in regions containing desmosomes, hemidesmosomes, and other types of adhesion sites (Green and Jones, 1990).

The overall organization of cytoskeletal IF networks, as well as their in vitro properties, suggests that they link the nuclear and cell surfaces and that they are involved in numerous cell functions, including the maintenance of the overall integrity of cytoplasm (Janmey et al., 1991; Wang et al., 1993) and cell shape (Goldman and Knipe, 1973). These latter roles are supported by the finding that some blistering skin diseases are caused by point mutations in keratins that have been related to structural alterations in IF, changes in the shape of individual keratinocytes, and the loss of mechanical properties of skin (Coulombe et al., 1991; Chipev et al., 1992; Fuchs and Coulombe, 1992; Lane et al., 1992; Steinert et al., 1994). The resistance to breakage of vimentin IF under conditions of high strain in vitro also supports their role in providing cells with resilience to mechanical stress in vivo (Janmey et al., 1991).

Based on their mechanical properties, as well as their insolubility in vitro, IF have long been thought to be very stable cytoskeletal elements relative to other cytoskeletal systems such as microtubules or microfilaments (Skalli et al., 1992). However, it has recently been shown that, at least in actively growing cultured cells, IF are in fact very dynamic structures in vivo. For example, at the posttranslational level, polymerized vimentin and keratin IF can incorporate microinjected unpolymerized subunits in living fibroblasts and epithelial cells (Vikstrom et al., 1989; Miller et al., 1993). Experiments involving FRAP also demonstrate that a steady state equilibrium exists between soluble IF subunits and polymerized IF in several cell types (Vikstrom et al., 1992; Okabe et al., 1993). These in vivo studies of IF dynamics have also been supported by fluorescence energy transfer experiments carried out in vitro (Angelides et al., 1989). Furthermore, it has been shown that IF exhibit rapid organizational and biochemical changes following various stimuli such as heat shock (Welch and Suhan, 1985), phosphorylation after exposure to growth factors (Baribault et al., 1989), and the transient association of IF with protein kinase C in response to a signal at the cell surface (Spudich et al., 1992). These findings have implicated IF in dynamic roles in several physiological activities, including signal transduction (Skalli et al., 1992).

Address all correspondence to Robert D. Goldman, Department of Cell and Molecular Biology, Northwestern University Medical School, 303 East Chicago Avenue, Chicago, IL 60611.

1. *Abbreviation used in this paper*: IF, intermediate filaments.

Numerous other properties of IF also reflect their dynamic nature. For example, biochemical- and metabolic-labeling studies suggest that IF protein synthesis occurs continuously and that newly synthesized subunits are incorporated into IF at both the co- and posttranslational levels (Isaacs et al., 1989; Ngai et al., 1990; Sarria et al., 1990). However, the pools of soluble subunits, whether they are newly synthesized or not, are very small, as indicated by the fact that the vast majority of IF protein is pelletable in cell-free preparations (Skalli et al., 1992). Other evidence supporting the dynamic nature of IF assemblies in vivo comes from transient transfection studies that demonstrate that the insertion of mutant polypeptide chains into endogenous polymerized networks have disruptive effects leading to their disassembly (Albers and Fuchs, 1989).

There is considerable evidence in support of a role for phosphorylation in regulating at least some of the dynamic properties of IF in vivo (Skalli et al., 1992). This evidence includes the finding that the hyperphosphorylation of IF proteins is accompanied frequently by their disassembly. For example, during mitosis in many types of eukaryotic cells, nuclear breakdown is accompanied by the hyperphosphorylation and coincident disassembly of the Type V IF polymer, the nuclear lamins (Moir and Goldman, 1993). In BHK-21 cells, it has been shown that vimentin IF disassemble during mitosis and that this alteration in the state of polymerization is regulated by phosphorylation (Chou et al., 1990; Chou et al., 1996). In other cell types, a more localized disassembly of cytoskeletal IF due to phosphorylation appears to take place in the cleavage furrow during cytokinesis (Nishizawa et al., 1991). In addition, it has been shown that vimentin IF are rapidly hyperphosphorylated and disassembled in cells exposed to phosphatase inhibitors, suggesting that IF assembly states in interphase cells are regulated by kinase/phosphatase equilibria (Eriksson et al., 1992*a*). In vitro studies support these in vivo observations, as numerous kinases phosphorylate and disassemble IF in cell-free preparations (for a review, see Skalli et al., 1992; Eriksson et al., 1992*b*).

Other evidence supporting the dynamic properties of IF has been derived from the use of synthetic peptides whose sequences are derived from the highly conserved 2B rod domain segment of keratin IF chains. In vitro, these peptides have been shown to interfere with keratin IF assembly and to promote the disassembly of preformed IF (Hatzeld and Weber, 1992; Kouklis et al., 1993; Steinert et al., 1993*c*). In addition, it has been observed that synthetic peptides corresponding to the 1A rod domain segment (or helix initiation region) (Steinert et al., 1993*a*; Steinert et al., 1993*c*) and the H1 subdomain immediately before the beginning of the 1A segment of Type II keratins (Chipev et al., 1992; Steinert and Parry, 1993) also interfere with keratin IF assembly and structure in vitro. These in vitro studies are of interest because they represent the first report of reagents that can alter IF structure under nondenaturing conditions. A logical extension of these studies is to determine whether these peptides may also be used to manipulate the dynamic properties of IF in vivo. To this end, we have developed procedures for testing the use of specific IF peptides to study the functions of IF in live cells. In this study, we present experimental evidence that 1A peptides alter the state of assembly of vimentin IF after their microinjection into cultured cells. The consequences of this disruption of IF in vivo are very substantial in that they lead to significant alterations in cell shape, the general organization and integrity of the cytoplasm, and the destabilization of other cytoskeletal systems. The results indicate that these reagents can be used as reversible inhibitors of IF structure and function.

Materials and Methods

Vimentin IF Assembly Assays In Vitro

Human vimentin was produced in *Escherichia coli* and purified by a combination of column chromatography and assembly/disassembly in vitro (see Chou et al., 1996). The purified protein was stored frozen (−80°C) in unpolymerized form in 2 mM phosphate buffer. For assembly of IF, frozen aliquots of the protein were precipitated at pH 5.0 with 0.1 M sodium acetate and subsequently dissolved in a solution containing 8 M urea, 25 mM Tris-HCl, pH 7.6, 5 mM DTT, and 1 mM EDTA. Vimentin IF were assembled from this solution at a concentration of 0.5 mg/ml by dialysis against vimentin IF assembly buffer (AB) containing 10 mM triethanolamine-HCl, pH 8.0, and 0.15 M KCl (Steinert et al., 1993*b*). In some experiments, aliquots of vimentin at the same concentration were dialyzed against AB devoid of KCl. Under these conditions, the protein did not assemble into IF but rather remained in the form of small oligomers (Steinert et al., 1981; Steinert et al., 1993*b*).

Synthetic Peptides

The following peptides were synthesized and purified by HPLC using established procedures (Chipev et al., 1992; Steinert et al., 1993*a*). These peptides were derived from the published sequences (single letter amino acid code) for human vimentin (Ferrari et al., 1986), human keratin 1 (Zhou et al., 1988), and human keratin 10 (Johnson et al., 1985). The residues were numbered according to the system of Conway and Parry (1988) as follows: vimentin 1A (residues 1–35): KVELQELNDRFANYIDKVRFLEQQNKILLAELEQL (~mol wt 4223); keratin 10 1A (residues 1–35): RVTQMNLNDRLASLYDKVRALEESNYELEGKIKEW (~mol wt 4140); keratin 10 1A (residues 1–18): RVTQMNLND**R**LASLYDKV (~mol wt 2136); and control keratin 10 1A (residues 1–18, mutant R10H; see Steinert et al., 1993*c*): RVTQMNLND**H**LASYLDKV (~mol wt 2118).

Following purification by HPLC, peptide concentrations were determined by amino acid analysis as previously described (Chipev et al., 1992; Steinert et al., 1993*a*). Peptides were stored in aliquots following lyophilization. Peptides were dissolved in the buffers described below for in vitro assembly/disassembly assays or in microinjection buffer (see below) for the in vivo assays just before use. Fresh aliquots of peptides were prepared at the beginning of each day.

IF Disassembly and Assembly Experiments Utilizing 1A Peptides In Vitro

The synthetic 1A peptides were dissolved in AB in order to achieve a final concentration of 2–3 mg/ml. Aliquots of peptides were then added to suspensions of polymerized vimentin IF (0.25 ml) so as to achieve 0.1–3-fold molar ratios. The reactions were allowed to proceed at room temperature and samples were taken at time intervals. In some cases, reactions between peptide and polymer were terminated by treatment with 0.7% aqueous uranyl acetate for negative staining and then examined by transmission electron microscopy (Steinert et al., 1993*a*). In other cases, the reactions were stopped by the addition of glutaraldehyde as a cross-linking agent at a final concentration of 0.05%. Cross-linking was allowed to proceed for 5 min at room temperature. Samples were then boiled in sample buffer used for polyacrylamide gel electrophoresis and aliquots were run on 3.75–17.5% gradient gels (Steinert et al., 1993*b*). In other experiments, peptides were added to oligomeric forms of vimentin in AB without KCl. After thorough mixing by mild mechanical agitation, KCl was added to a final concentration of 0.15 M to promote IF polymerization. During the assembly reaction, aliquots were removed at time intervals and examined

by electron microscopy and gel electrophoresis as previously described (Steinert et al., 1993*b*).

In vitro Assembly of Microtubules and F-Actin

For control experiments, tubulin was prepared from mouse brain tissue as described in Borisy et al. (1975) and retained in unpolymerized form in a buffer of 50 mM MES, pH 6.5, 1 mM EDTA, 0.5 mM $MgSO_4$. Assembly into microtubules in vitro was achieved upon addition of GTP to a final concentration of 0.5 mM at 37°C in the absence or presence of a 1–10-fold molar excess of the 1A peptides. Stock solutions of the peptides were dissolved at a concentration of 3 mg/ml in the same buffer.

Nonmuscle actin was prepared from new born mouse epidermis as described elsewhere (McGuire et al., 1977) and retained in the G-actin form at 0.5 mg/ml in a solution containing 2 mM Tris-HCl, pH 8.0, 0.2 mM ATP, 0.5 mM DTT, and 0.5 mM $CaCl_2$. The 1A peptides were dissolved in the same buffer and added at 1–10-fold molar ratios. Polymerization of actin in the absence or presence of the peptide was achieved by the addition of KCl to a final concentration of 0.2 M at room temperature. In some assays, F-actin was decorated with heavy meromyosin prepared from mouse skeletal muscle as described elsewhere (Ishikawa et al., 1969). The products of each assembly experiment were assayed by negative stain electron microscopy using 0.7% aqueous uranyl acetate.

Cell Culture

Baby hamster kidney fibroblasts (BHK-21) and mouse 3T3 fibroblasts were grown on etched grid "locator" coverslips (Bellco Biotechnology, Vineland, NJ) for microinjection studies as previously described (Vikstrom et al., 1989; Vikstrom et al., 1992). Fibroblasts devoid of vimentin and all other cytoskeletal IF proteins were obtained from 18-d-old vimentin knockout embryonic cultures (kindly provided by Drs. Charles Babinet and Emma Colucci-Guyon of the Pasteur Institute, Paris, France). These cells were grown in DME (Sigma Immunochemicals, St. Louis, MO) supplemented with 10% fetal calf serum (Hyclone Laboratories, Logan, UT) and antibiotics as previously described (Vikstrom et al., 1989). In some cases, colchicine (Sigma Immunochemicals) was added to 3T3 cells at a concentration of 7.5 μg/ml culture medium to disassemble microtubules.

Microinjection

Cells were microinjected with the 1A peptides dissolved in microinjection buffer (20 mM Tris, pH 8.0, 170 mM NaCl, 3 mM KCl) just before their use at final concentrations of 0.5–4.0 mg/ml. Microinjections were carried out on a Nikon inverted microscope (Melville, NY) equipped with either a Narishigi micromanipulator and injector (Greenvale, NY) or an Eppendorf Micromanipulator 5171 and Transjector 5246 (Fremont, CA), using glass needles as previously described (Vikstrom et al., 1989; Vikstrom et al., 1992). With the latter device, cells were injected at a pressure of 32 hPa.

The average volume of peptide solution injected per cell was determined using published procedures (Lee, 1989; Minaschek et al., 1989). This involved the establishment of a standard curve generated by measuring the diameter of spherical droplets containing 10 μg dextran-rhodamine (dextran, tetramethyl rhodamine, 70,000 mol wt [4.9 mol rhodamine per mol dextran]; Molecular Probes, Eugene OR) per ml injection buffer formed in Cargille Type FF immersion oil (R.P. Cargille Laboratories, Inc., Cedar Grove, NJ) and by determining the amount of fluorescence per droplet using the method described by Lee (1989). Fluorescence images of each droplet were captured as quickly as possible using a Hamamatsu camera (model C2400 SIT; Bridgewater, NJ) and were stored in Image I (Universal Imaging Corp. West Chester, PA.). The total fluorescence intensity was determined for each drop using the "calibrate total gray scale level" function. The volume for each droplet was determined by measuring its diameter with the Image I "measure with caliper" function. The resulting data were used to establish a standard curve for volume versus total fluorescence intensity (Lee, 1989). Subsequently, 3T3 or BHK cells grown on locator coverslips were microinjected with different concentrations of rhodamine-dextran in microinjection buffer using the Eppendorf system. Injected cells were first viewed with phase optics, and subsequently fluorescence images of live cells were "captured" as rapidly as possible and stored in Image I as described above. The Image I "measure area brightness" function was used to determine the total amount of fluorescence in each live cell. The results obtained following microinjection of three different concentrations of dextran-rhodamine into 175 cells showed that an average of 0.06 pl was delivered to each cell.

Quantitation of Cytoskeletal Proteins in BHK and 3T3 Cells

One dish of either confluent 3T3 or BHK cells was trypsinized, rinsed twice with PBS, and split into two conical tubes. The cells in one tube were resuspended in 2 ml of PBS, and the number of cells was determined with a hemocytometer. The other tube was centrifuged and resuspended in 0.5 ml of SDS gel electrophoresis sample buffer and used for SDS-PAGE and quantitative Western immunoblotting analyses as previously described (Wong and Cleveland, 1990). Since vimentin and actin are the most prominent bands in total cell lysates, their quantities were estimated by comparing densitometric scans of Coomassie blue–stained gel samples with different amounts of purified bacterially expressed human vimentin and chicken muscle actin (a gift of Dr. Rex Chisholm, Northwestern University, Chicago, IL) separated on the same gel. Gel scanning was carried out on an LKB 2222-010 UltroScan XL Densitometer (Pharmacia LKB Biotechnolgy Inc., Piscataway, NJ). The tubulin concentration in the cell lysates was obtained by immunoblotting with a monoclonal antibody (N357; Amersham Corp. Arlington Heights, IL). Purified 6x bovine brain tubulin (Vallee, 1986; a gift of Dr. Christine Collins, Northwestern University, Chicago, IL) was used as a standard in these assays.

Microscopy

After microinjection with a 1A peptide, cells on "locator" coverslips were fixed in methanol at −20°C for 5 minutes (Vikstrom et al., 1989) to visualize IF and microtubules. Upon removal from the methanol, cells were washed in PBS at room temperature and processed for indirect immunofluorescence (Vikstrom et al., 1989) using either a rabbit antibody (Yang et al., 1985) or a mouse monoclonal antibody directed against vimentin (Sigma Immunochemicals). In some experiments, the mouse monoclonal antitubulin (see above) was used to visualize microtubules, and rhodamine-phalloidin (Molecular Probes) was used to visualize actin. In the latter case, cells were fixed in PBS for 5 min at RT, followed by 3 min in 0.1% NP–40 in PBS and washing in PBS. Secondary antibodies included goat anti–rabbit TRITC and goat anti–mouse FITC (Kirkegaard and Perry Labs, Inc., Gaithersburg, MD). Double labeling was carried out as described elsewhere (Yang et al., 1985). After staining with antibodies, coverslips were mounted in gelvatol (Yang et al., 1985) and examined with either a Zeiss LSM2 Confocal or Axiophot microscope (Thornwood, NY). Images were recorded on 35 mm film for conventional fluorescence or on an optical disk for confocal observations (Moir et al., 1994). A Phillips 400 TEM (Mahwah, NJ) was used to examine the negative stain preparations and electron micrographs were taken on Kodak film (Rochester, NY).

Results

1A Peptides Interfere with Vimentin IF Assembly and Structure In Vitro

When the 35-residue vimentin 1A peptide (See Materials and Methods) is added to a suspension of preformed IF in a 1:1 molar ratio in IF assembly buffer (AB), disassembly of the IF into small particles is seen within 30 min at room temperature. The overall structural features of this disassembly process can be monitored by taking samples from a reaction mixture at time intervals and preparing them for negative stain electron microscopy (Fig. 1, *A–D*). In parallel experiments using identical conditions, glutaraldehyde cross-linking demonstrates that the large oligomeric protein complexes corresponding to intact IF are reduced to smaller oligomers containing primarily one to four protein chains (Fig. 2). Taken together, the electron microscopic and cross-linking assays show that the 1A peptide induces the disassembly of vimentin IF in vitro. We have also carried out the reverse experiment to examine the assembly of vimentin IF in the presence of the vimentin 1A peptide.

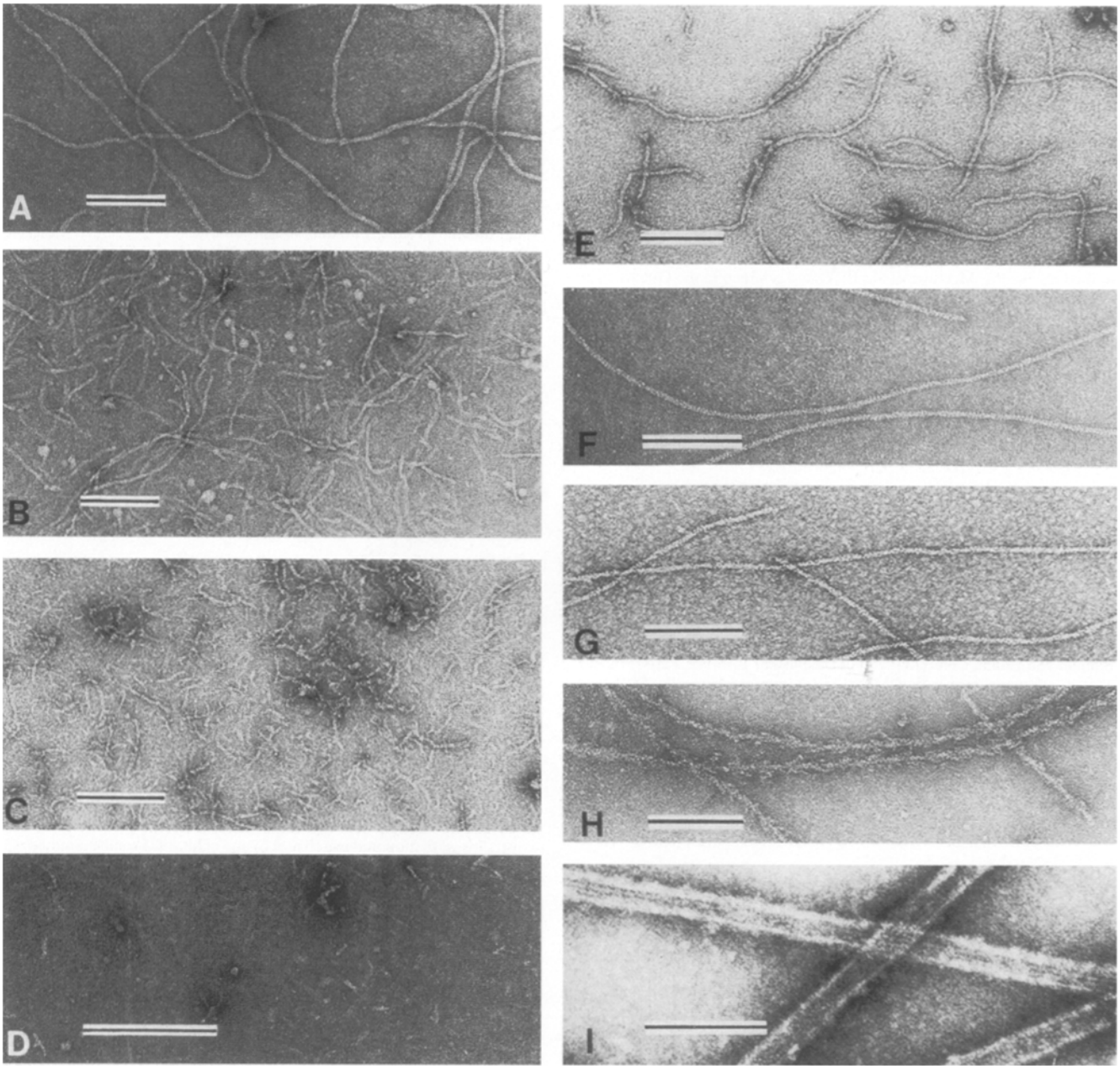

Figure 1. Electron microscopic analysis of the effects of the vimentin 1A peptide on polymerized vimentin IF. (*A*) Preformed vimentin IF in the absence of peptide. (*B–D*) Effects on vimentin IF after the addition of the 1A peptide at 1:1 molar ratios: (*B*) 5 min, (*C*) 10 min, (*D*) 30 min. (*E*) Effects of the 18-residue mutant R10H keratin 10 1A peptide on vimentin IF after 30 min. (*F–H*) Effects of the peptide on F-actin: (*F*) actin filaments in the absence of 1A peptide and (*G*) actin filaments assembled in the presence of a 3:1 molar ratio of 1A peptide: F-actin; (*H*), same as (*G*) followed by the addition of murine skeletal muscle heavy meromyosin. (*I*) Effects of a 3:1 molar ratio of vimentin 1A peptide: tubulin. The peptide was added prior to the polymerization of microtubules. Negatively stained with 0.7% uranyl acetate. (*A–H*) Bar, 200 nm; (*I*) Bar, 100 nm.

The results show that vimentin oligomers maintained in low ionic strength buffers (AB devoid of KCl, see Materials and Methods) rapidly assemble into IF upon the addition of KCl to 0.15 M (Steinert et al., 1981; Steinert et al., 1993*a*). However, in the presence of a 1:1 molar ratio of peptide 1A, the assembly process is inhibited, resulting in the conversion of the predominantly tetrameric form of vimentin in solution to largely monomeric vimentin (data not shown). Identical disassembly or assembly inhibition reactions are seen using the morphological and cross-linking assays with both full-length (35 residues) or half-length (18 residues) wild-type keratin 10 1A peptides at 1:1 molar ratios (data not shown).

The fact that the inhibitory action of the 1A peptide on vimentin IF is retained in the first 18 residues of this sequence is consistent with similar studies on keratin IF (Steinert et al., 1993*c*). On the other hand, the control keratin 10 1A peptide bearing an arginine to histidine (R10H) substitution corresponding to a major site of mutation in either the keratin 10 or 14 chains, which causes epider-

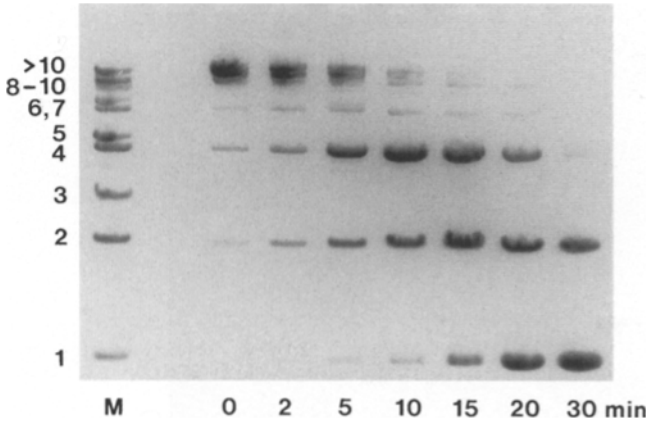

Figure 2. SDS-PAGE analyses of the disassembly of preformed vimentin IF after mixing with 1:1 molar ratios of the vimentin 1A peptide. Aliquots were removed at the times indicated. These were immediately cross-linked with glutaraldehyde. Molecular weight markers (*M*) using cross-linked keratin 10 chains (60-Kd) as previously described (Steinert et al., 1993*a*). Numbers at left refer to the size of oligomers. The large oligomeric products corresponding to cross-linked intact vimentin IF at "0" time were reduced to mostly single chains, dimers, and small oligomers within 30 min (Steinert et al., 1993*b*).

molytic hyperkeratosis or epidermolysis bullosa simplex (Steinert et al., 1993*c*), respectively, has comparatively much less of an effect on the morphology of preformed vimentin IF at molar ratios of 1:1 (Fig. 1 *E*). The only apparent morphological alteration, even at 10-fold molar ratios of mutant peptide, is a "rougher" appearance at the surface of IF perhaps revealing a slight "unraveling" of protofilaments. At these same molar ratios, no obvious changes in vimentin IF assembly or disassembly reactions could be detected by turbidity, cross-linking, or sedimentation analyses. The latter revealed that about 95% of the total protein remained pelletable. These results are similar to those obtained with keratin IF in vitro (Steinert et al., 1993*c*).

In further control experiments, we determined the overall in vitro assembly properties of the other major cytoskeletal proteins, microtubules and actin filaments, in the presence of the wild-type and mutant 1A peptides. Assembly of murine epidermal G-actin into F-actin was unaffected by the inclusion of up to a 3:1 molar ratio of the wild-type vimentin 1A peptide (compare Figs. 1, *F* and *G*). The subsequent decoration of the peptide-treated F-actin by heavy meromyosin yielded the typical arrowhead configurations, indicating that the ability of F-actin to bind myosin was unimpaired (compare Figs. 1, *G* and *H*). Similarly, over 90% of murine brain tubulin that assembled into microtubules in vitro was unaltered by inclusion of either the vimentin (Fig. 1 *I*), the full-length, or the mutant keratin 10 1A peptides (not shown) at molar ratios of 3:1 (also assayed by turbidity; Steinert et al., 1993*c*). At molar ratios exceeding 3:1, the yield of tubulin or actin in polymerized structures began to decrease slightly, and at 10:1 ratios, approximately 50% of these proteins remained polymerized. At molar ratios exceeding 5:1, the peptides interfered significantly with the buffering capacity of the solutions used for tubulin and actin assembly, which may help to explain the observed in vitro effects on microtubules and actin filaments. Together, these observations on microtubule and F-actin assembly in vitro, as well as the limited inhibitory effect of the mutant peptide on vimentin assembly in vitro, further emphasize that the 1A peptide has very specific effects on IF assembly and structure. These data are of special significance when viewed in light of the measured amounts of tubulin and actin in cells relative to the amounts of microinjected peptide (see below).

Microinjection of the 1A Peptides into Living Cells

BHK-21 and 3T3 cells contain an extensive cytoplasmic network of polymerized Type III IF. In BHK cells, these networks consist mainly of vimentin with a lesser amount of desmin (Quinlan and Franke, 1982). In 3T3 cells, only vimentin can be detected. Cells on locator coverslips were injected with several concentrations of the various 1A peptides dissolved in injection buffer and fixed for indirect immunofluorescence with vimentin antibody at time intervals after injection. At concentrations below 0.5 mg/ml, no obvious effects could be detected with the vimentin 1A peptide. In the 0.5–2.0 mg/ml range, BHK cells exhibited a variety of changes ranging from very subtle to more obvious. The majority of injected cells showed small alterations in shape that were correlated with a localized conversion of the IF staining pattern from a more filamentous state to a more diffuse one, within 15-60 min post-injection. These changes in IF structure were especially evident at the cell periphery and were coincident with varying degrees of retraction of the cell borders (data now shown).

More rapid, obvious, and consistent changes were seen in the majority of BHK cells after microinjection of the vimentin 1A peptide at concentrations of 2–4 mg/ml. The extensive cytoplasmic IF networks normally seen by indirect immunofluorescence with vimentin antibody (Fig. 3 *A*), changed within minutes after microinjection. Initially, the normal IF pattern was altered to a less filamentous state (Fig. 3, *B* and *C*), subsequently appearing to become fragmented into bright spots, short rod-like structures, and irregularly shaped structures within 15–30 min (Fig. 3, *D* and *E*). The latter patterns vary from cell to cell. Ultimately, all cells look approximately the same, as these various vimentin-rich structures aggregate near the nucleus coincident with alterations in their shape from a fully spread configuration to a rounded one (Fig. 3 *F*). Similarly, individual live cells followed by phase contrast during this IF disassembly process dramatically alter their shape from the typical asymmetric configuration of a fully spread fibroblast to a cell with a rounded morphology (Fig. 4, *A–C*). The latter cells frequently exhibit extensive surface blebbing (Fig. 4 *D*). A variable fraction of these rounded cells lose their adhesions to their substrates and float away, and others that are tenuously adherent to the coverslips are lost during fixation and processing for indirect immunofluorescence. However, the majority remain following fixation and processing. Of 319 cells injected, 80% appeared as in Fig. 4, *C* and *D*. Other cells showed varying responses, most likely due to variations in the amount of peptide injected. (See Minaschek et al., 1989 for a detailed discussion of the difficulties involved in the in-

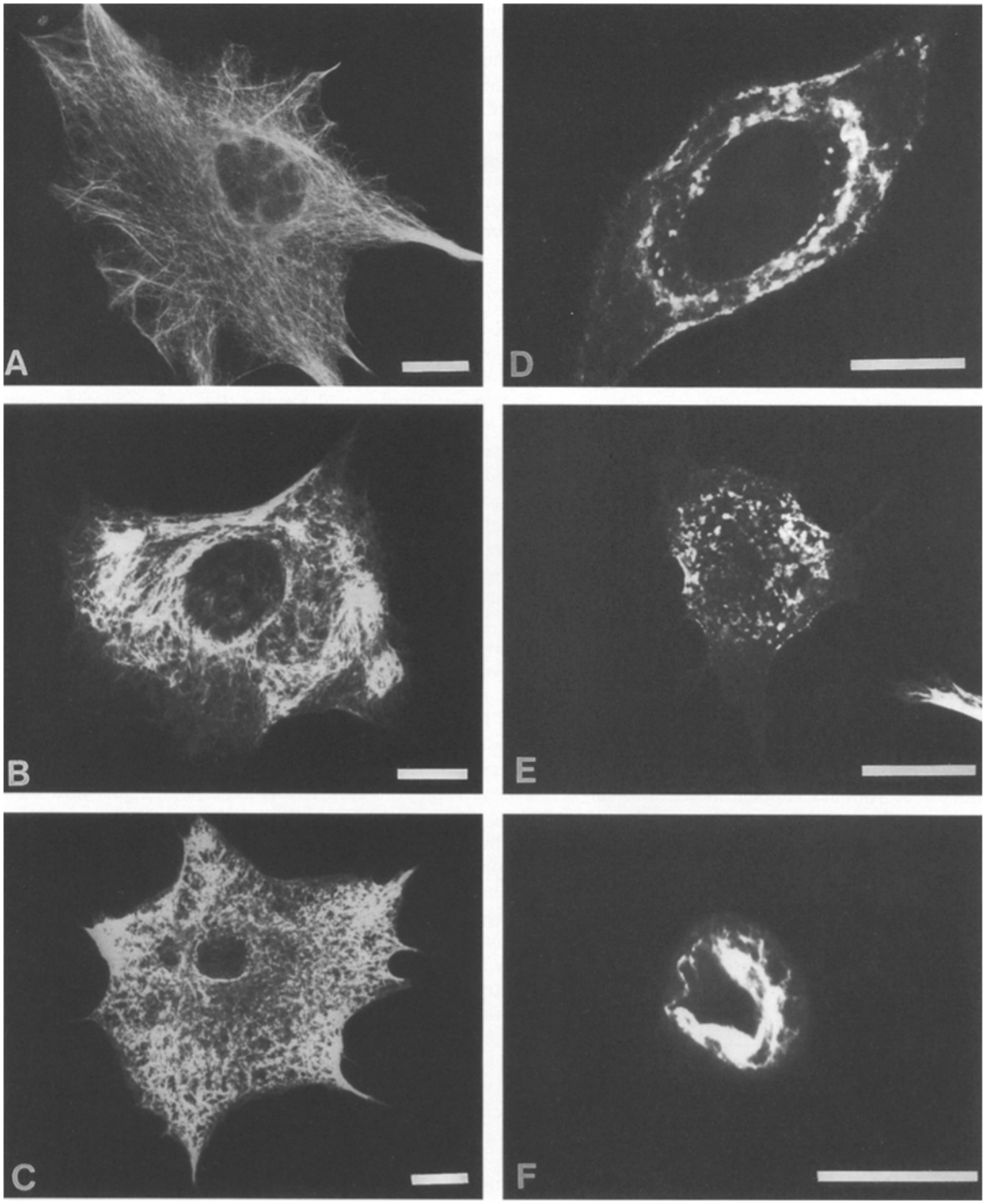

Figure 3. (*A*) Uninjected BHK-21 cell fixed and stained for indirect immunofluorescence with vimentin antibody. (*B–F*) BHK cells observed at approximately 15 (*B*), 20 (*C*), 30 (*D*), 45 (*E*), and 60 (*F*) min after injection with the vimentin 1A peptide. All cells fixed and stained for indirect immunofluorescence with vimentin antibody. Bars, 25 μm.

jection of known amounts of solutions into cells.) Identical results were obtained for 3T3 cells, which were more sensitive to the peptides. Maximum effects on IF network disassembly and cell shape were seen in 15–30 min at concentrations of 0.5–2.0 mg/ml (data not shown as the cells appear identical to those seen in Fig. 3). The effects on 3T3 cells were reproducible within the same time frame as observed for BHK cells. At a concentration of 0.5–2.0 mg/ml, 90% (n = 137) of the 3T3 cells appeared as in Fig 4, *C* and *D*.

After 1–3 h, cells which had been induced to round-up after injection of the peptide began to recover their normal morphology, and this was coincident with the reappearance of normal IF networks. Initially, this rapid reversal made it difficult to determine the more dramatic effects

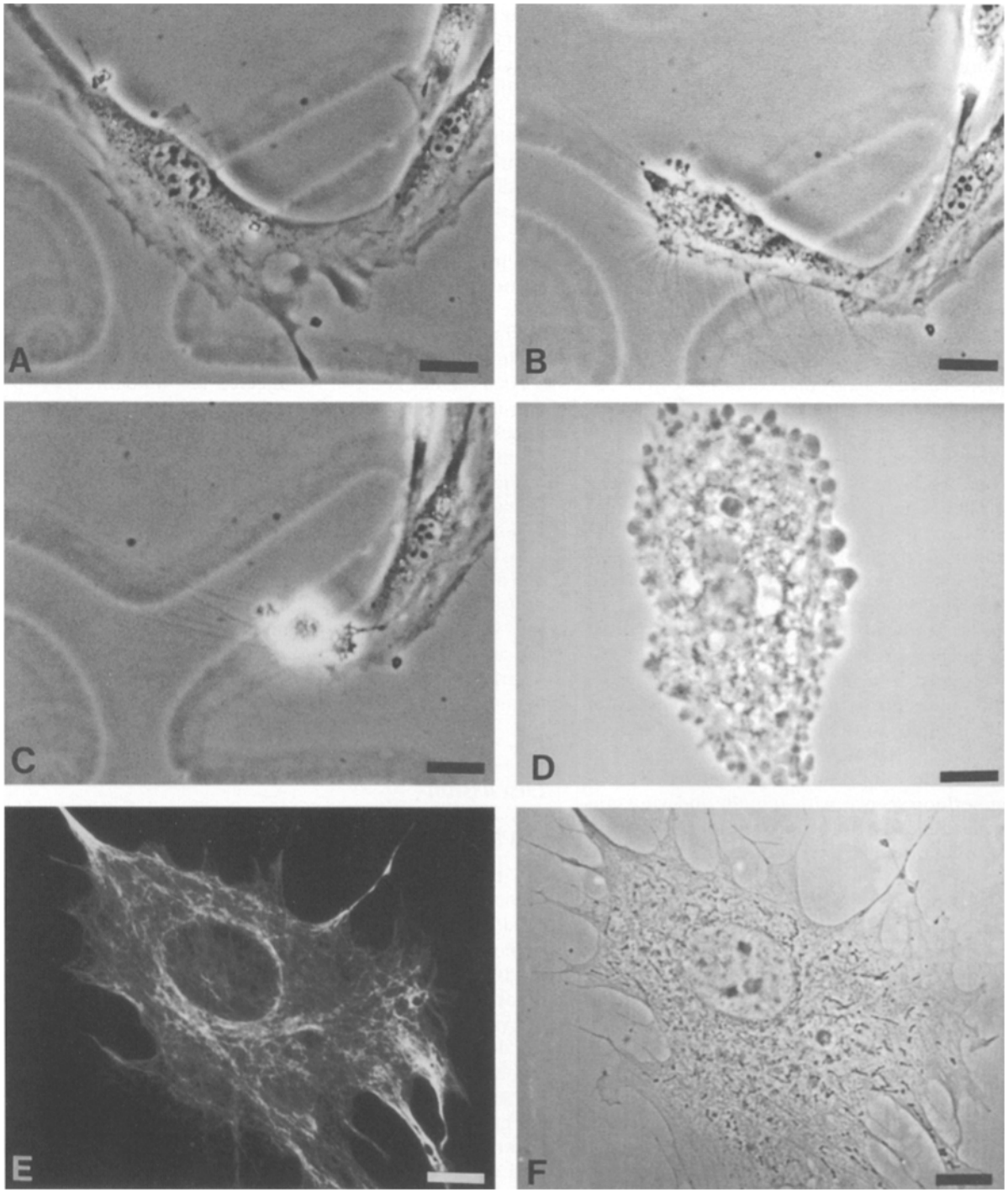

Figure 4. (*A–C*) A series of micrographs of a live 3T3 cell before injection (*A*), 20 min after injection (*B*), and 30 min after injection (*C*) as seen by phase contract optics. (*D*) By 30–45 min, the majority of cells appear rounded and exhibit extensive surface blebbing. (*E* and *F*) The same cell observed at 4 h after injection of the vimentin 1A peptide. This cell had rounded up and then respread on the coverslip. Subsequently it was fixed and stained for indirect immunofluorescence with vimentin antibody. (*A–C*, *E*, and *F*) Bars, 25 μm; (*D*) Bar, 5 μm.

of the peptide injections because our pilot experiments involved monitoring cells beginning at 1 h after injection. Recovery of normal IF networks and cell shape was observed between 3–6 h after injection (Fig 4, *E* and *F*).

A series of microinjection experiments were also carried out with the other 1A peptides (see Materials and Methods). Both the wild-type keratin 10 1A full-length and half-length peptides were equally effective at concentrations of 2–4 mg/ml in BHK cells and 0.5–2 mg/ml in 3T3 cells. The cells exhibited changes that were indistinguishable from those seen with the vimentin 1A peptide (see Figs. 3 and 4). As a control, the keratin 10 1A peptide bearing the single amino acid substitution R10H (see Materials and Methods) was microinjected at the same concentrations into

BHK and 3T3 cells. No obvious effects on IF organization or cell shape could be detected for up to 2–4 h of observation after injection (not shown because injected cells possess IF patterns similar to those seen in Fig. 3 *A*).

Due to the dramatic effects of the wild-type 1A peptides on IF assembly and cell shape, we also carried out observations on the other major cytoskeletal systems, microtubules and actin-containing microfilaments. Indirect immunofluorescence revealed that microtubules decreased in number coincident with the alterations in the IF network and cell shape. Only a few short microtubules (or none at all) could be resolved in rounding up BHK or 3T3 cells observed at 30 min after the microinjection of the vimentin 1A peptide at concentrations of 2–4 mg/ml or 0.5–1 mg/ml, respectively. In the rounded cells, small spots surrounded by a diffuse fluorescence background could be seen as detected by indirect immunofluorescence with tubulin antibody (Figs. 5, *A–C*). In the case of actin-containing microfilaments, stress fibers appeared to disassemble into large fluorescent aggregates as cell rounding progressed (Figs. 5, *D–F*). These effects on microtubule and microfilament patterns were also reversed within a few hours. Based on morphological criteria, their reassembly also appeared to be coincident with the reestablishment of cell shape and the normal appearance of the IF network. In the case of cells injected with the mutant peptide, no obvious alterations in the distribution of microtubules or microfilaments were seen at the concentrations tested.

Several additional controls for the specific binding of the vimentin 1A peptides to IF and not to microtubules or microfilaments were undertaken. Cells were observed at short time intervals after injection and processing for double-label immunofluorescence with tubulin and vimentin antibodies. Typically, after 5–15 min, the peripheral regions of cells were devoid of IF, but extensive arrays of microtubules remained (Fig. 5, *G* and *H*). This suggested that the effect of the peptide was to first destabilize vimentin IF and subsequently to destabilize the microtubules remaining in the peripheral regions of the cytoplasm. 3T3 cells were also treated with colchicine for short time intervals in order to disassemble microtubules. After 30 min of colchicine treatment, these cells retained a network of IF, most of which remained dispersed between the nucleus and the cell surface. These cells contained very few assembled microtubules, and they remained well spread on the substrate with little or no obvious change in shape (Fig. 6, *A–C*). When injected with the 1A peptide in the concentration range of 0.5–2 mg/ml, the cells rapidly disassembled their IF networks and rounded up in the same fashion as seen in Figs. 3 and 4 (data not shown).

Since the injection of the 1A peptides had pleiotropic effects in live cells, especially with respect to alterations in the other cytoskeletal systems, it became important to estimate the relative amounts of peptide injected per cell compared to the endogenous concentrations of vimentin, actin, and tubulin. To this end, we have approximated the in vivo molar ratios by first calculating that the average volume of solution injected into 3T3 and BHK cells is .06 pl (see Materials and Methods). In the case of 3T3 cells, injection at a concentration of 0.5 mg/ml vimentin 1A peptide is equivalent to 0.007 fmol per cell. We have calculated that there is an average of 0.153 fmol vimentin, 0.007 fmol tubulin, and 0.443 fmol actin per 3T3 cell. Therefore the molar ratios of peptide/cytoskeletal protein are 1:20 for vimentin, 1:1 for tubulin, and 1:64 for actin. For the shorter peptides, the molar ratios at the same concentration of 0.5 mg/ml would be approximately 1:10 for vimentin, 2:1 for tubulin, and 1:32 for actin. A concentration of 2 mg/ml vimentin 1A peptide is equivalent to 0.028 fmol per cell, yielding approximate peptide/cytoskeletal protein molar ratios of 1:5 for vimentin, 4:1 for tubulin, and 1:16 for actin. A similar range of molar ratios relative to average amounts of injected peptides was obtained for BHK cells. However, these cells require more peptide to achieve the same in vivo results. This appears to be accounted for by the fact that in BHK cells, there is about 30–40% more IF protein due to the presence of desmin (data not shown).

As a further control, we injected the vimentin 1A peptide into vimentin-free fibroblasts derived from vimentin knockout mice (Fig. 7, *A* and *B*). At concentrations of 0.5–1.0 mg/ml of the vimentin 1A or the two K10 1A peptides, no significant alterations in cell shape could be detected in injected cells. A few cells showed partial retraction in the region of the needle puncture immediately following injection, but 85% ($n = 221$) retained their shape with no obvious alterations in either microtubule or actin-stress fiber arrays (Fig. 7, *C* and *D*). Unlike normal fibroblasts, these cells were extremely fragile and great care had to be taken for successful injections. These observations further demonstrate the specific targeting of the 1A peptides to intermediate filaments and not other cytoskeletal constituents.

Discussion

In Vitro Studies

In vitro studies demonstrate that at 1:1 molar ratios, helix initiation 1A peptides induce the rapid and efficient conversion of polymerized IF into small oligomeric and monomeric protein chains, using either the vimentin or keratin 10 1A peptides. The finding that both vimentin and keratin 1A peptides are equally effective in depolymerizing vimentin IF is most likely related to the fact that the 1A domain is one of the most highly conserved domains involved in IF structure (Steinert et al., 1993*a*; Steinert et al., 1993*c*; Parry and Steinert, 1995). The specificity of these effects on IF in vitro is supported by experiments with the keratin 10 mutant 1A peptide containing a single amino acid substitution, R10H. At the same or excess ratios of mutant peptide to vimentin IF, relatively little effect on IF structure is detected. The findings that wild-type or mutant peptides only induce significant microtubule or F-actin structural changes at high molar excesses support their use as specific disruptors of IF structure in vivo.

Presumably, the peptides act by binding to the same sequences on the intact protein chains comprising polymerized IF, thereby causing destabilization and eventual collapse of IF structure. Interestingly, the 1A helix initiation peptide is more destructive in vitro than the 2B helix termination peptide and about as equally destructive as the H1 peptide in the case of keratin IF (Chipev et al., 1992). However, the H1 peptide has little or no effect on vimentin IF in vitro or in vivo (data not shown), in sharp contrast

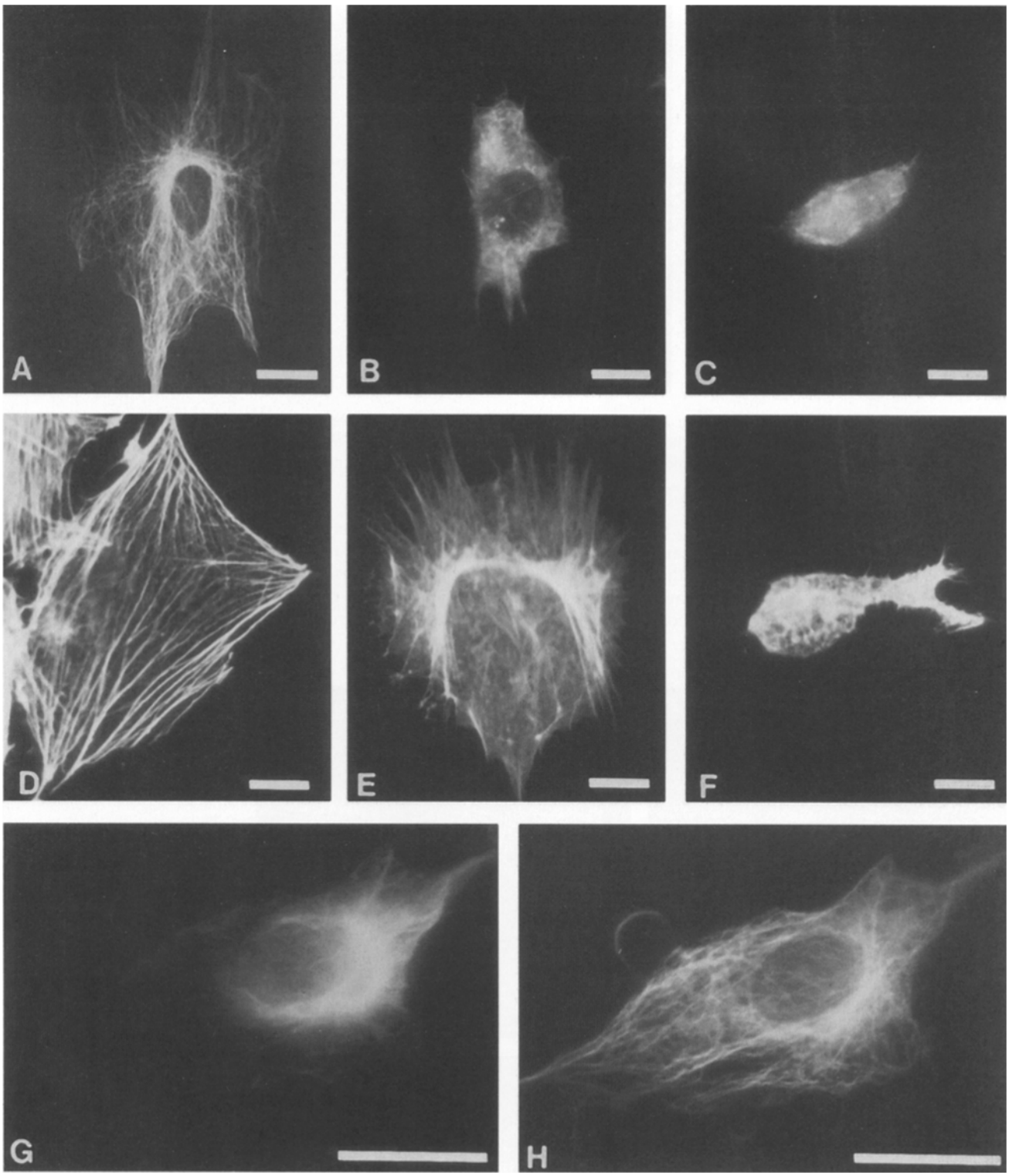

Figure 5. (*A–C*) Indirect immunofluorescence observations of microtubule patterns in BHK cells before (*A*) and at time intervals following microinjection with peptide 1A: (*B*) 15 min, and (*C*) 30 min. (*D–F*) Fluorescence observations of changes in actin patterns as cells round up after microinjection with 1A peptide. Cells were fixed and stained with rhodamine-phalloidin. Note conversion of prominent stress fibers into a primarily diffuse pattern. (*D*) Before injection, (*E*) 15 min after injection, and (*F*) 45 min after injection. (*G–H*) BHK cell observed at 5 min after injection and subsequently fixed and double labeled with vimentin (*G*) and tubulin (*H*) antibodies. Note that the majority of vimentin antibody staining has disappeared to the left of the nucleus in *G*, while numerous microtubules are seen in the same region. Bars, 25 μm.

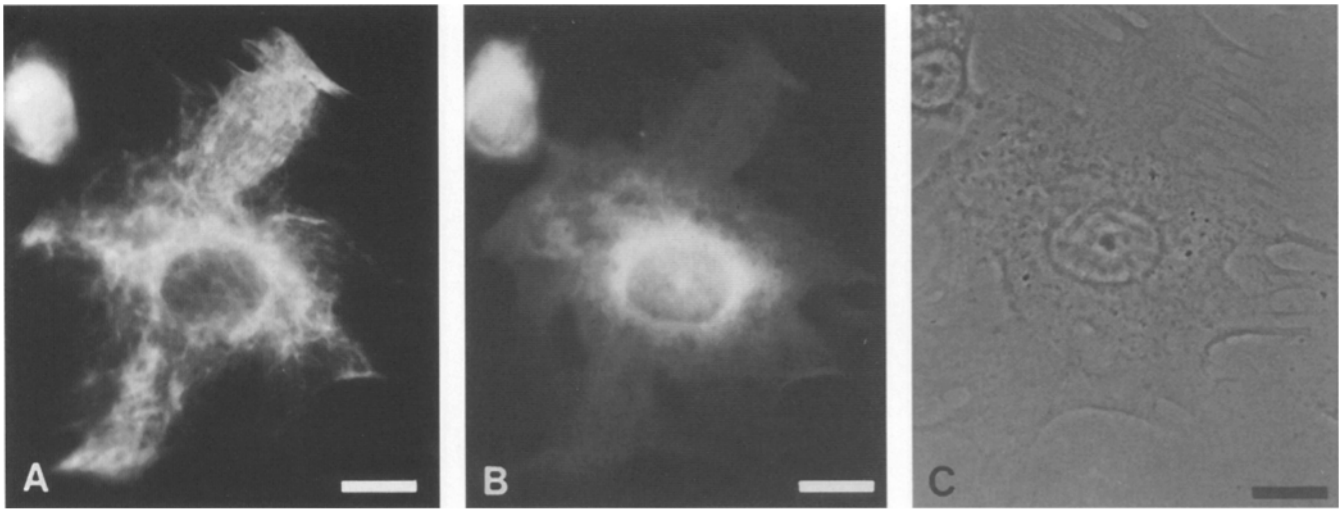

Figure 6. BHK cell treated with colchicine for 30 min and then fixed and stained for double indirect immunofluorescence with vimentin antibody (*A*) and tubulin antibody (*B*). (*C*) The same cell in phase contrast. Note that the overall shape and the degree of cell spreading is not altered significantly in the absence of microtubules. Bars, 25 μm.

to its effect on keratin IF (Chipev et al., 1992). Other mimetic peptides derived from other domains of keratin IF polypeptide chains have also been studied in vitro, but most have not been effective in inducing IF disassembly (Steinert et al., 1993*a*). Although the use of a variety of mimetic peptides has provided important insights into IF structure in vitro, many of the peptides studied to date are not particularly useful for in vivo studies as they must be used at excessive molar ratios of peptide to polymer. It is precisely for this reason that we have chosen the helix ini-

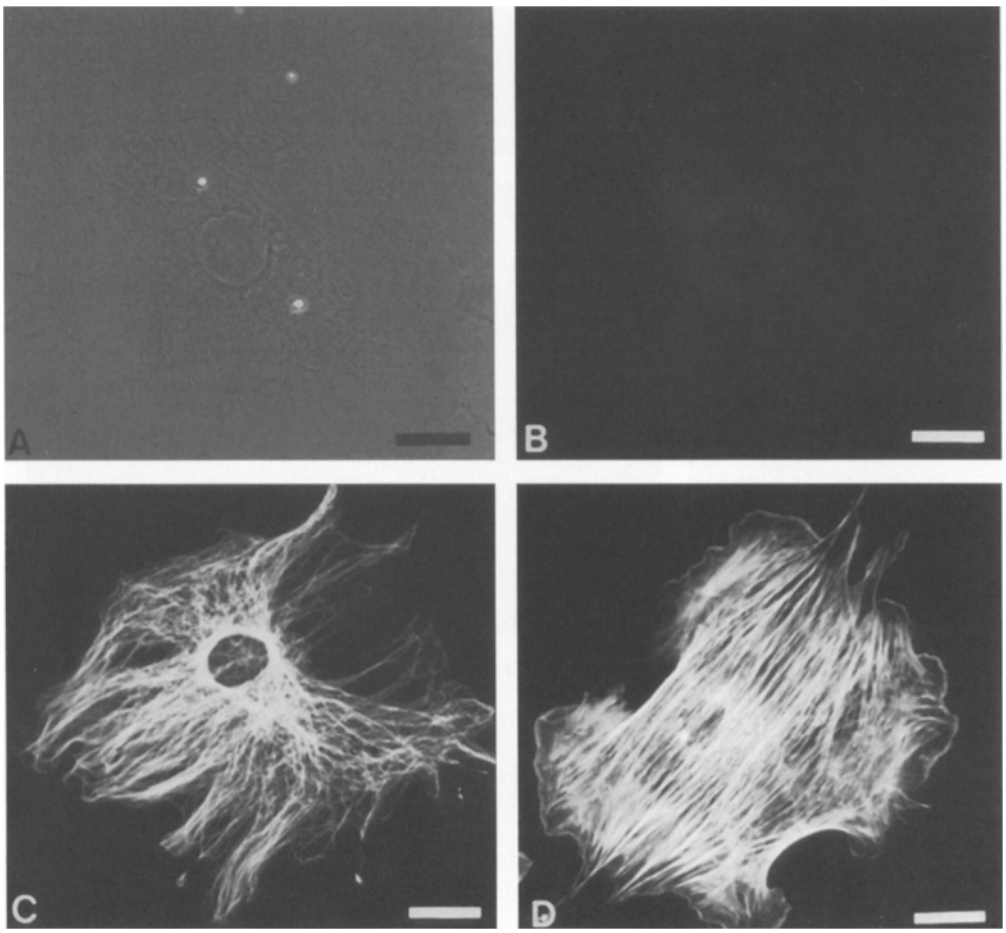

Figure 7. (*A* and *B*) Same vimentin-free cell observed with phase contrast (*A*) and fluorescence optics (*B*). The cell was fixed and stained for indirect immunofluorescence with vimentin antibody. (*C*) Cell observed at 45 min after injection with 1A peptide following fixation and staining with antitubulin. (*D*) Cell observed at 45 min after injection of 1A peptide following fixation and staining with rhodamine phalloidin. Bars, 25 μm.

tiation 1A peptides for in vivo studies, as they appear to be the most potent at the lowest molar ratios tested in vitro (Steinert et al., 1993*c*).

In Vivo Studies

The rationale for the in vivo studies stems from recent evidence demonstrating that IF exist in a state of dynamic equilibrium (Vikstrom et al., 1992; Miller et al., 1993). This suggests that we should be able to use the 1A peptides to bind and "capture" exchangeable subunits, rendering them nonexchangeable and thereby acting as targeted disruptors of IF structure. The microinjection results described in this study support this contention.

A major concern regarding the use of the peptides is related to their concentrations in vivo after microinjection. Even though the 1A peptide effects can be titered precisely in vitro, it is difficult to determine equivalent molar ratios in vivo, because of the inherent inaccuracies of the microinjection procedure. However, the finding that the average effective peptide concentrations required for IF disruption in vivo are equivalent to less than the 1:1 molar ratios used in vitro supports their specificity and targeting to IF. Further support for the targeting of the 1A peptide primarily to IF and not to microtubules or microfilaments is derived both from the results with colchicine-treated cells and the rapid response of IF to the 1A peptides shortly after microinjection when microtubules and microfilaments appear to remain intact (see Figs. 5, *G* and *H*, and 6). The controls employing the mutant peptide and the lack of response in the vimentin free fibroblasts also support the use of the 1A peptides as inhibitors of IF structure and function. Most likely, the peptides disrupt IF structure in vivo by the breakage of IF polymers into oligomeric complexes. In support of this, electron microscopic observations indicate that relatively very few intact IF can be seen in 3T3 cells at 30 min after injection of the vimentin 1A peptide (unpublished observations).

Other approaches have also been used to perturb IF networks in vivo (see Introduction). These include colchicine treatment (Goldman and Knipe, 1973; Green and Goldman, 1986; Yang et al., 1992), antivimentin injections (Klymkowsky, 1981), heat shock (Welch and Suhan, 1985), the microinjection of protein kinase A (Lamb et al., 1989), and the microinjection of kinesin antibodies (Gyoeva and Gelfand, 1991). In each of these experimental situations, vimentin IF are reorganized within the cytoplasm to form large aggregates, but they appear to remain polymerized and cell shape is not significantly altered. On the other hand, the disassembly of vimentin IF with the 1A peptides does have a dramatic effect on cell shape, the overall integrity of other cytoskeletal systems, and the adhesive properties of cells. Further support for the role of IF in cell shape and adhesion is derived from studies of blistering diseases of the skin in which keratinocytes alter their shape and intercellular contacts in concert with the occurrence of keratin mutations that induce the clumping and breakage of bundles of keratin-IF (Anton-Lamprecht, 1983; Williams and Elias, 1987; Coulombe et al., 1991; Ishida-Yamamoto et al., 1991, 1992). The majority of these mutations are in the 1A helix initiation region (Fuchs et al., 1994; Steinert et al., 1994; Parry and Steinert, 1995). A role for glial IF in cell shape has also been demonstrated in cultured astrocytes (Weinstein et al., 1991).

The importance of cytoskeletal IF in maintaining cytoplasmic and mechanical integrity is supported by in vitro analyses demonstrating that the viscoelastic properties of vimentin IF are distinctly different from those exhibited by microtubules and F-actin (microfilaments). Comparative studies show that vimentin IF are unique in that they are less rigid at low strain and become much more rigid at high strain forces that disrupt F-actin and microtubules (Janmey et al., 1991). It is due to this property of "hardening" at high strains that has led to the conclusion that IF are the cytoskeletal elements most responsible for the maintenance of "cell integrity" (Janmey et al., 1991). The fact that the vimentin-free cells used in this study appear to be extremely fragile with respect to their ability to tolerate a micropuncture also supports this possibility.

The changes in cell shape accompanying the peptide-induced disassembly of vimentin IF networks are also intriguing in light of the coincident destabilization of microtubules and microfilaments. Since the minimum effective doses of peptide used in vivo are below those required to obtain significant changes in microtubule and/or F-actin polymerization in vitro, it appears likely that the disruption of vimentin IF leads to the destabilization of the other cytoskeletal constituents.

The destabilization of other cytoskeletal components is not surprising if one considers the morphological, physiological, and biochemical data supporting associations between microtubules and IF (for reviews see Goldman, 1971; Goldman et al., 1980; Yang et al., 1992) and between microfilaments and IF (Hubbard and Lazarides, 1979; Green et al., 1986). For example, microtubules exist in parallel and most likely cross-bridged arrays in fibroblasts (Goldman and Knipe, 1973) and in neurons (Runge et al., 1981). Furthermore, virtually all inhibitors which disassemble microtubules also induce the reorganization of vimentin and other Type III IF (see e.g., Goldman, 1971; Yang et al., 1992), indicating that these two cytoskeletal systems are interactive. These interactions may involve IF-associated proteins (IFAPs; Yang et al., 1992), microtubule-associated and motor proteins (LeTerrier et al., 1982; Bloom and Vallee, 1983; Gyoeva and Gelfand, 1991), as well as direct interactions between IF subunit proteins, such as Type IV NF-H, and microtubules (Hisanaga et al., 1993). Interactions between IF and microfilaments have been described in detail in cultured cells (Green et al., 1986; Hollenbeck et. al., 1989). In support of this, it appears that the COOH-terminal domain of vimentin can associate with actin (Cary et al., 1994), and a gene has been described that encodes a protein with potential actin and IF-binding domains (Brown et al., 1995).

Based on the apparent importance of the expression of vimentin in early development (Tapscott et al., 1981) and the deleterious effects seen in transgenic mice which overexpress vimentin (Capetanaki et al., 1989), it is surprising that no obvious phenotypes have been reported in vimentin gene knockout mice (Colucci-Guyon et al., 1994). There are no straightforward explanations for this result. However, it is possible that one cytoskeletal system might be able to compensate for another, at least to an extent necessary for overall cell survival. An indication that this

might be the case comes from the observation of the fibroblasts of the vimentin-free mouse used in this study. These cells contain remarkably complex arrays of microtubules and actin-containing stress fibers for early passage embryonic cultures (Fig. 7). Further support for the existence of cytoskeletal compensation is derived from the observation that after colchicine treatment, there is an increase in the number and prominence of stress fibers (Goldman, 1971; unpublished observations) and that tubulin expression is upregulated in mice lacking the NF-L gene (Julien, J.P., personal communication). Furthermore, the finding that the vimentin-free fibroblasts are extremely fragile with respect to microinjection suggests that the mechanical properties of these cells are abnormal. In this regard, more extensive studies determining the viscoelastic properties of live vimentin-free cells should be undertaken (see Wang et al., 1993). Alterations in such properties are to be expected from the in vitro analyses of the mechanical properties of IF relative to other cytoskeletal polymers (Janmey et al., 1991).

In summary, we have presented evidence that the 1A helix initiation peptides are useful tools for the disruption of vimentin IF both in vitro and in vivo. The data presented demonstrate that in cells which express vimentin, the resulting IF polymer plays central and important roles in cell shape, in the maintenance of the overall integrity of cytoplasm, and in stabilizing cytoskeletal interactions and cell substrate adhesions. We are now using these and other mimetic peptides to attempt to delve into the functions of other IF systems. The preliminary results in epithelial cells containing keratin and in neurons containing Type IV neurofilaments indicate that the use of peptides targeted to specific subdomains of IF will continue to provide very important insights into their specific functions in living cells.

We wish to thank Dr. Gary Borisy of the University of Wisconsin for discussing with us the quantitative aspects of microinjection methodology. We also thank Laura Davis for help in preparing this manuscript.

This work was generously supported by a grant from the National Institute of General Medical Sciences.

Received for publication 1 August 1995 and in revised form 29 April 1996.

References

Albers, K., and E. Fuchs. 1989. Expression of mutant keratin cDNA in epithelial cells reveals possible mechanisms for initiation of assembly of intermediate filaments. *J. Cell Biol.* 108:1477–1493.

Angelides, K.J., K.E. Smith, and M. Takeda. 1989. Assembly and exchange of intermediate filament proteins of neurons: neurofilaments are dynamic structures. *J. Cell Biol.* 108:1495–1506.

Anton-Lamprecht, I. 1983. Genetically induced abnormalities of epidermal differentiation and ultrastructure in ichthyoses and epidermolyses: pathogenesis, heterogeneity, fetal manifestation and prenatal diagnoses. *J. Invest. Dermatol.* 81:149s–156s.

Baribault, H., R. Blouin, L. Bourgon, and N. Marceau. 1989. Epidermal growth factor-induced selective phosphorylation of cultured rat hepatocyte 55kD cytokeratin before filament reorganization and DNA synthesis. *J. Cell Biol.* 109:1665–1676.

Bloom, G.S., and R.B. Vallee. 1983. Association of microtubule associated protein 2 MAP2 with microtubules and intermediate filaments in cultured brain cells. *J. Cell Biol.* 96:1523–1531.

Borisy, G.G., J.M. Marcum, J.B. Olmsted, D.B. Murphy, and K.A. Johnson. 1975. Purification of tubulin and associated high molecular weight proteins from porcine brain and characterization of microtubule assembly in vitro. *Ann. NY Acad. Sci.* 253:107–123.

Brown, A., G. Bernier, M. Mathieu, J. Rossant, and R. Kothary. 1995. The mouse dystonia musculorum gene is a neural isoform of bullous pemphigoid antigen 1. *Nat. Genet.* 10:301–306.

Capetanaki, Y.G., S. Starnes, and S. Smith. 1989. Expression of the chicken vimentin gene is transgenic mice: efficient assembly of the avian protein into the cytoskeleton. *Proc. Natl. Acad. Sci. USA.* 86:4884–4886.

Cary, R.B., M.W. Klymkowsky, R.M. Evans, A. Domingo, J.A. Dent, and L.E. Backhus. 1994. Vimentins tail interacts with actin-containing structures in vivo. *J. Cell Sci.* 107:1609–1622.

Chipev, C.C., B.P. Korge, N. Markova, S. Bale, J.J. DiGiovanna, J.G. Compton, and P.M. Steinert. 1992. A leucine → proline mutation in the H1 subdomain of keratin 1 causes epidermolytic hyperkeratosis. *Cell.* 70:821–828.

Chou, Y.-H., J.R. Bischoff, D. Beach, and R.D. Goldman. 1990. Intermediate filament reorganization during mitosis is mediated by $p34^{cdc2}$ phosphorylation of vimentin. *Cell.* 62:1063–1071.

Chou, Y.-H., P. Opal, R.A. Quinlan, and R.D. Goldman. 1996. The relative roles of specific N- and C-terminal phosphorylation sites in the disassembly of intermediate filament in mitotic BHK-21 cells. *J. Cell Sci.* 109:817–826.

Colucci-Guyon, E., M.M. Portier, I. Dunia, D. Paulin, S. Pournin, and C. Babinet. 1994. Mice lacking vimentin develop and reproduce without an obvious phenotype. *Cell.* 79:679–694.

Conway, J.F., and D.A.D. Parry. 1988. Intermediate filament structure. 3. Analysis of sequence homologies. *Int. J. Biol. Macromol.* 10:79–98.

Coulombe, P.A., M.E. Hutton, R. Vassar, and E. Fuchs. 1991. A function of keratins and a common thread among different types of epidermolysis bullosa simplex diseases. *J. Cell Biol.* 115:1661–1674.

Eriksson, J.E., D.L. Brautigan, R. Vallee, J. Olmsted, H. Fujiki, and R.D. Goldman. 1992*a*. Cytoskeletal integrity in interphase cells requires protein phosphatase activity. *Proc. Natl. Acad. Sci. USA.* 89:11093–11097.

Eriksson, J.E., P. Opal, and R.D. Goldman. 1992*b*. Intermediate filament dynamics. *Curr. Opin. Cell Biol.* 4:99–104.

Ferrari, S., R. Battini, L. Kaczmarek, S. Rittling, B. Calbretta, J.K. deRiel, V. Philiponis, J.-F. Wei, and R. Baserga. 1986. Coding sequence and growth regulation of the human vimentin gene. *Mol. Cell Biol.* 6:3614–3620.

Fuchs, E., and P.A. Coulombe. 1992. Of mice and men: genetic skin diseases of keratin. *Cell.* 69:899–902.

Fuchs, E., P. Coulombe, J. Cheng, Y. Chan, E. Hutton, A. Snyder, L. Degenstein, Yu-Q.-C., A. Letai, and R. Vassar. 1994. Genetic basis of epidermolysis bullosa simplex and epidermolytic hyperkeratosis. *J. Invest. Dermatol.* 103:25s–30s.

Goldman, R.D. 1971. The role of three cytoplasmic fibers in BHK-21 cell motility. I. Microtubules and the effects of colchicine. *J. Cell Biol.* 51:752–762.

Goldman, R.D., and D.W. Knipe. 1973. Functions of cytoplasmic fibers in nonmuscle cell motility. *Cold Spring Harbor Symp. Quant. Biol.* 37:523–534.

Goldman, R.D., B. Hill, P. Steinert, M. Whitman, and R.V. Zackroff. 1980. Intermediate filament-microtubule interactions: evidence in support of a common organization center. *In* Microtubules and Microtubule Inhibitors. Debrabander and DeMey, editors. Elsevier-North Holland, Netherlands. 91–102.

Green, K., and R.D. Goldman. 1986. Evidence for an interaction between the cell surface and intermediate filaments in cultured fibroblasts. *Cell Motil. & Cytoskeleton.* 6:389–405.

Green, K.J., and J.C.R. Jones. 1990. Interaction of intermediate filaments with the cell surface. *In* Cellular and Molecular Biology of Intermediate Filaments. R.D. Goldman, and P.M. Steinert, editors. Plenum Press, New York. 147–174.

Green, K.J., J.C. Talian, and R.D. Goldman. 1986. Relationship between intermediate filaments and microfilaments in cutlured fibroblasts is evidence for common foci during cell spreading. *Cell Motil. Cytoskeleton.* 6:406–418.

Gyoeva, F.K., and V.I. Gelfand. 1991. Co-alignment of vimentin intermediate filaments with microtubules depends on kinesin. *Nature (Lond.).* 353:445–448.

Hatzfeld, M., and K. Weber. 1992. A synthetic peptide representing the consensus sequences motif at the carboxyl-terminal end of the rod domain inhibits intermediate filament assembly and disassemble preformed filaments. *J. Cell Biol.* 116:157–166.

Hisanaga, S., S. Yasugawa, T. Yamakawa, E. Miyamoto, M. Ikebe, M. Uchiyama, and T. Kishimoto. 1993. Dephosphorylation of microtubule binding sites at the neurofilament-H tail domain by alkaline, acid and protein phosphatases. *J. Biochem.* 113:705–709.

Hollenbeck, P.J., A.D. Bershadsky, O.Y. Pletijushkina, I.S. Tint, and J.M. Vasiliev. 1989. Intermediate filament collapse in an ATP-dependent and actin-dependent process. *J. Cell Sci.* 92:621–631.

Hubbard, B., and E. Lazarides. 1979. Co-purification of actin and desmin from chicken smooth muscle and their co-polymerization in vitro to intermediate filaments. *J. Cell Biol.* 80:166–182.

Isaacs, W.B., R.K. Cook, J.C. Van Atta, C.M. Redmon, and A.B. Fulton. 1989. Assembly of vimentin in cultured cells varies with cell types. *J. Biol. Chem.* 264:17953–17960.

Ishida-Yamamoto, A., J.A. McGrath, S.J. Chapman, I.M. Leigh, and E.B. Lane. 1991. Epidermolysis bullosa simplex Dowling-Meara Type is a genetic disease characterized by an abnormal keratin filament network involving keratins K5 and K14. *J. Invest. Dermatol.* 97:959–968.

Ishida-Yamamoto, A., J.A. McGrath, M.R. Judge, I.M. Leigh, E.B. Lane, and R.A.J. Endy. 1992. Selective involvement of keratin K1 and Keratin K10 in the cytoskeletal abnormality of epidermolytic hyperkeratosis bullous congenital ichthyosiform erythroderma. *J. Invest. Dermatol.* 99:19–26.

Ishikawa, H., R. Bischoff, and H. Holtzer. 1969. Formation of arrowhead complexes with heavy meromyosin in a variety of cell types. *J. Cell Biol.* 43: 312–328.

Janmey, P.A., U. Enteneuer, P. Traub, and M. Schliwa. 1991. Viscoelastic properties of vimentin compared with other filamentous biopolymer networks. *J. Cell Biol.* 113:155–160.

Johnson, L.D., W.W. Idler, X.M. Zhou, D.R. Roop, and P.M. Steinert. 1985. Structure of a gene for the human epidermal keratin of 67,000Da. *Proc. Natl. Acad. Sci. USA.* 82:1896–1900.

Klymkowsky, M. 1981. Intermediate filaments in 3T3 cells collapse after intracellular injection of a monoclonal anti-intermediate filament antibody. *Nature (Lond.).* 291:249–251.

Kouklis, P.D., P. Traub, and S.D. Georgatos. 1993. Involvement of the consensus motif at coil 2b in the assembly and stability of vimentin intermediate filaments. *J. Cell Sci.* 102:31–41.

Lamb, N.S.C., A. Fernandez, J.R. Feramisco, and W.J. Welch. 1989. Modulation of vimentin containing intermediate filament distribution and phosphorylation in living fibroblasts by the cAMP-dependent protein kinase. *J. Cell Biol.* 108:2409–2422.

Lane, E.B., E.K. Rugg, H. Nausaria, I.M. Leigh, A.H.M. Heagerty, A. Ishida-Yamamoto, and R.A.J. Eady. 1992. A mutation in the conserved helix termination peptide of keratin 5 in hereditary skin blistering. *Nature (Lond.).* 356: 244–246.

Lee, G.M. 1989. Measurement of volume injected into individual cells by quantitative fluorescence microscopy. *J. Cell Sci.* 94:443–447.

LeTerrier, J.F., R.K.H. Liem, and M.L. Shelanski. 1982. Interactions between neurofilaments and microtubule-associated proteins: a possible mechanism for intraorganellor bridging. *J. Cell Biol.* 95:982–986.

McGuire, J., E. Lazarides, and A. DiPasquale. 1977. Actin is present in mammalian keratinocytes. *In* Biochemistry of Curtaneous Epidermal Differentiation, M. Seiji, and I.A. Bernstein, editors. Tokyo University Press, Tokyo, Japan. 69–80.

Miller, R.K., S. Khuon, and R.D. Goldman. 1993. Dynamics of keratin assembly: exogenous Type I keratin rapidly associates with Type II keratin in vivo. *J. Cell Biol.* 122:123–135.

Minaschek, G., J. Bereiter-Hahn, and G. Berthold. 1989. Quantitation of the volume of liquid injected into cells by means of pressure. *Exp. Cell Res.* 183: 434–442.

Moir, R., and R.D. Goldman. 1993. Lamin dynamics. (ed. Ron Evans and John Newport). *Curr. Opin. Cell Biol.* 5:408–411.

Moir, R.D., M. Lowy-Montag, and R.D. Goldman. 1994. Dynamic properties of nuclear lamins: lamin B is associated with sites of DNA replication. *J. Cell Biol.* 125:1201–1212.

Ngai, J., T.R. Coleman, and E. Lazarides. 1990. Localization of newly synthesized vimentin subunits reveals a novel mechanism of intermediate filament assembly. *Cell.* 60:415–427.

Nishizawa, K., T. Yano, M. Shibata, S. Endo, S. Saga, T. Takahashi, and M. Inagaki. 1991. Specific localization of phosphointermediate filament protein in the constricted area of dividing cells. *J. Biol. Chem.* 266:3074–3079.

Okabe, S., H. Muyasaka, and N. Hirokawa. 1993. Dynamics of the neuronal intermediate filaments. *J. Cell Biol.* 121:375-386.

Parry, D.A.D., and P.M. Steinert. 1995. Intermediate filament structure. Molecular Biology Intelligence Unit. R.G. Landis Co., Austin, TX.

Quinlan, R., and W. Franke. 1982. Heteropolymer filaments of desmin and vimentin in vascular smooth muscle tissue and cultured baby hamster kidney cells demonstrated by chemical crosslinking. *Proc. Natl. Acad. Sci. USA.* 79: 3452–3456.

Runge, M.S., T.M. Lane, D.A. Yphantis, M. Lifsics, A. Saito, M. Altin, K. Reimke, and R.C. Williams Jr. 1981. ATP-induced formation of an associated complex between microtubules and neurofilaments. *Proc. Natl. Acad. Sci. USA.* 78:1431–1435.

Sarria, A.J., S.E. Nordeem, and R.M. Evans. 1990. Regulated expression of vimentin cDNA in the presence and absence of pre-existing vimentin filament network. *J. Cell Biol.* 111:553–565.

Skalli, O., and R.D. Goldman. 1991. Recent insights into the assembly, dynamics, and function of intermediate filament networks. *Cell Motil. Cytoskeleton.* 19:67–69.

Skalli, O., Y.-H. Chou, and R.D. Goldman. 1992. Intermediate filaments: not so tough after all. *Trends Cell Biol. 2:308–312.*

Spudich, A., T. Meyer, and L. Stryer. 1992. Association of the beta isoform of protein kinase C with vimentin filaments. *Cell Motil. & Cytoskeleton.* 22: 250–256.

Steinert, P.M., W.W. Idler, F. Cabral, M.M. Gottesman, and R.D. Goldman. 1981. *In vitro* assembly of homopolymer and copolymer filaments from intermediate filament subunits of muscle and fibroblastic cells. *Proc. Natl. Acad. Sci. USA.* 78:3692–3696.

Steinert, P.M., and D.A.D. Parry. 1993. The conserved H1 domain of the Type II keratin 1 chain plays an essential role in the alignment of nearest-neighbor molecules in mouse and human keratin 1/keratin 10 intermediate f filaments at the two-to-four molecule level of structure. *J. Biol. Chem.* 268:2878–2887.

Steinert, P.M., L. Marekov, R.D.B. Fraser, and D.A.D. Parry. 1993*a*. Keratin intermediate filament structure: crosslinking studies yield quantitative information on molecular dimensions and mechanism of assembly. *J. Mol. Biol.* 230:436–452.

Steinert, P.M., L.N. Marekov, and D.A.D. Parry. 1993*b*. Diversity of intermediate filament structure: evidence that the alignment of coiled-coil molecules in vimentin is different from that in keratin intermediate filaments. *J. Biol. Chem.* 268:24916–24925.

Steinert, P.M., J.M. Yang, S.J. Bale, and J.G. Compton. 1993*c*. Concurrence between the molecular overlap regions in keratin intermediate filaments and the location of keratin mutations in genodermatoses. *Biochem. Biophys. Res. Comm.* 197:840–848.

Steinert, P.M., A.C.T. North, and D.A.D. Parry. 1994. Structural features of keratin intermediate filaments. *J. Invest. Dermatol.* 103:19s–24s.

Tapscott, S.F., J.S. Bennett, Y. Toyama, F. Kleinbart, and H. Holtzer. 1981. Intermediate filament proteins in the developing chick spinal cord. *Dev. Biol.* 86:40–54.

Valle, R.B. 1986. Reversible assembly purification of microtubules without assembly-promoting agents and further purification of tubulin, microtubule-associated proteins, and MAP fragments. *Methods Enzymol.* 134:89–104.

Vikstrom, K.L., G.G. Borisy, and R.D. Goldman. 1989. Dynamic aspects of intermediate filament networks in BHK-21 cells. *Proc. Natl. Acad. Sci. USA.* 86:549–553.

Vikstrom, K.L., S.S. Lim, R.D. Goldman, and G.G. Borisy. 1992. Steady state dynamics of intermediate filament networks. *J. Cell Biol.* 118:121–129.

Wang, N., J.P. Butler, and D.E. Ingber. 1993. Mechanotransduction across the cell surface and through the cytoskeleton. *Science (Wash. DC).* 260:1124–1127.

Weinstein, D.E., M.L. Shelanski, and R.K.H. Liem. 1991. Suppression by antisense mRNA demonstrates a requirement for the glial fibrillary acidic protein in the formation of stable astrocytic processes in response to neurons. *J. Cell Biol.* 112:1205–1213.

Welch, W.J., and J.P. Suhan. 1985. Morphological study of the mammalian stress response: characterization of changes in cytoplasmic organelles, cytoskeleton, and nucleoli, and appearance of intranuclear actin filaments in rat fibroblasts after heat-shock treatment. *J. Cell Biol.* 101:1198–1211.

Williams, M.L., and P.M. Elias. 1987. Genetically transmitted, generalized disorders of cornification. *The Ichthyoses Dermatologic Clinics.* 5:155–178.

Wong, P.C., and D.W. Cleveland. 1990. Characterization of dominant and recessive assembly-defective mutations in mouse meurofilament NF-M. *J. Cell Biol.* 111:1987–2003.

Yang, H.-Y., N. Lieska, A.E. Goldman, and R.D. Goldman. 1985. A 300,000-mol-wt intermediate filament-associated protein in baby hamster kidney BHK-21 cells. *J. Cell Biol.* 100:620–631.

Yang, H.-Y., N. Lieska, A. Goldman, and R.D. Goldman. 1992. Colchicine-sensitive and colchicine-insensitive intermediate filament systems distinguished by a new intermediate filament-associated protein, IFAP-70/280kD. *Cell Motil. Cytoskeleton.* 22:185–199.

Zhou, X.M., W.W. Idler, D.R. Roop, A.C. Steven, and P.M. Steinert. 1988. The sequence and structure of human keratin 10: organization and possible structures of end domain sequences. *J. Biol. Chem.* 263:15584–15589.